

An Investigation of Refrigerant Void Fraction in Horizontal, Microfin Tubes

D.A. Yashar
D.M. Graham

M.J. Wilson
J.C. Chato

H.R. Kopke
T.A. Newell

A series of experiments to determine void fraction in both condensation and evaporation have been performed in horizontal microfin tubes with refrigerants R134a and R410A. Mass flux varied from 75 kg/m²·s to 700 kg/m²·s and average test section quality varied from 5% to 80%. Zero degree (axial grooving) and 18 degree helix microfin tube configurations have been examined in both condensation and evaporation. Four tubes were examined (7.3 mm and 8.9 mm diameters with axial and 18 degree helix angle microfins). Evaporation and adiabatic conditions in microfin tubes generally show similar void fraction trends found in smooth tubes. Condensation results for microfin tubes show a lower void fraction than smooth tubes.

INTRODUCTION

Prediction of void fraction in refrigeration tubing is important for three reasons. First, void fraction allows the refrigerant charge to be determined in an evaporator and condenser. Second, when two of the three terms of the “triangle” relationship between mass flux/quality, void fraction, and pressure drop, are known the remaining factor can be determined. Third, void fraction prediction can be used as an important parameter for prediction of heat transfer as demonstrated by Traviss, et al. (1973).

Internally enhanced “microfin” tubes have been adopted by industry over the past two decades. The refrigeration industry has implemented many types of internally enhanced tubes as empirical evidence has shown significant performance advantages over smooth tubes (Chiang, (1993). While a significant amount of work has been performed on the heat transfer and pressure drop characteristics in microfin tubing (Newell and Shah 1999), very little information has been available on void fraction characteristics of microfin tubing. As discussed by Newell and Shah (1999), “microfin” or “microgroove” tubes are defined as tubes in which the fin height or groove depth is generally smaller than the average thickness of the liquid film on the inside surface of the tube. Japanese literature has often referred to the tubes as “microgroove” while others tend to refer to the tubes as “microfin”. This paper will use the term “microfin”.

Microfin tube heat transfer enhancement is often similar to the surface area fractional increase added to the tube wall. Heat transfer can be enhanced significantly beyond the tube surface area enhancement when the fin structures also act to change the flow field configuration, such as helping to wet the upper tube wall in evaporation when operating in dryout conditions. In a contrasting nature, as shown by Graham, et al. (1998a), flow conditions can occur where the heat transfer enhancement is only a small fraction of the surface area fraction increase.

This investigation builds on the smooth tube, refrigerant void fraction work of Graham, et al. (1998a). The smooth tube results form a reference base for examining the characteristics of internally enhanced tubes in evaporation and condensation. Internal “microfin” enhancements

John C. Chato is a professor emeritus, **Ty A. Newell** is an associate professor and **Michael J. Wilson** is a Ph.D. candidate in the Mechanical and Industrial Engineering Department at the University of Illinois at Urbana-Champaign. **David A. Yashar** is an engineer at the National Institute of Standards and Technology, U.S. Department of Commerce. **Helmut R. Kopke** is an engineer with Sargent and Lundy, Inc. **Douglas M. Graham** is an engineer with Proctor and Gamble Corp.

generally enhance heat transfer more than the commonly associated increase in pressure drop. For example, Graham, et al. (1999) demonstrated that axial and helical microfin tubes have very different, but generally significant heat transfer enhancement characteristics. Pressure drop characteristics for axial and helical microfin tubes showed relatively small, but similar, changes in pressure drop relative to smooth tube pressure drop. The primary reason for the observed characteristics is speculated to be the separation of the liquid film regions that affect heat transfer and pressure drop. Heat transfer resistance is primarily buried in the viscous sublayer and buffer regions of the interaction between the vapor core and the liquid film adjacent to the wall/microfin surfaces. Pressure drop, however, is primarily caused by the interaction between the vapor core and the liquid film's turbulent layer that is above the viscous sublayer and buffer region. Hurlburt and Newell (1999) theoretically predict the thickness of these layers and the relative thermal resistances in the liquid film region.

BACKGROUND

Rice (1987) reviewed many void fraction models and described the differences and similarities of the prediction methods relative to common refrigerants. The comparison reveals a wide level of uncertainty when void fraction models derived from work based on non-refrigerant fluids, geometries, and flow conditions are applied to common refrigerant conditions. Graham, et al. (1998b); Kopke, et al. (1998); Wilson, et al. (1998); and Yashar, et al. (1998) examined ten existing void fraction models relative to their experimental void fraction results for refrigerants. The specifics of the model agreements will not be discussed here, but some of the general characteristics of void fraction modeling will be described.

Many void fraction models may be categorized into two primary groups. One group consists of models that extend the simple homogenous flow model. The second group is characterized by correlations primarily based on the Lockhart-Martinelli parameter that makes use of the unique relation between a two-phase flow and the characteristics of the individual single phase flows. A number of other void fraction models are available that are based on a variety of parameters. Collier (1980) provides a good description of some of these models and experiments.

Homogenous void fraction models tend to be built from a basic model in which the liquid and vapor phases travel together at a common velocity.

$$\alpha = \frac{1}{\left(\frac{1-x}{x}\right)\left(\frac{\rho_g}{\rho_l}\right)} \quad (1)$$

Assuming a difference in bulk velocity of each phase, a slip velocity can be introduced.

$$\alpha = \frac{1}{\left(\frac{1-x}{x}\right)\left(\frac{\rho_g}{\rho_l}\right)S} \quad (2)$$

Various mechanisms have been devised for calculating a slip velocity. Zivi (1964) used a minimization of entropy generation argument to determine a slip ratio related to the density ratio of the phases. Rigot (1973) made the simple assumption of a constant slip velocity value. Smith (1969) derived a slip velocity model based on the liquid and vapor having the same velocity pressure. Additionally, a tuning factor to account for a fraction of liquid entrained in the core and the remaining liquid fraction separated from the vapor flow was assumed. A model by Ahrens (1983) based on steam/water data from Thom (1964) derived a slip velocity with depen-

dence on phase viscosities and densities. A common feature of all these models is a lack of mass flux dependence.

Lockhart-Martinelli void fraction models are generally based on the correlation parameter, X_{tt} , which is the square root ratio of the liquid-only pressure gradient to the vapor-only pressure gradient. Models based on the Lockhart-Martinelli parameter are often characterized as ones in which viscous dissipation, such as in the annular flow regime, are dominant. Usually, the “ tt ” (turbulent liquid-turbulent vapor) form of the X parameter is used. Substituting expressions for single phase, turbulent pressure drop of each pure phase results in a simple expression for X_{tt} .

$$X_{tt} = \left(\frac{1-x}{x}\right)^{0.9} \left(\frac{\rho_g}{\rho_l}\right)^{0.5} \left(\frac{\mu_l}{\mu_g}\right)^{0.1} \quad (3)$$

Wallis (1969) formulated a void fraction expression based on a simple curvefit with X_{tt} dependence. Domanski (1983) adjusted Wallis’s model for X_{tt} values larger than 10. Baroczy (1965) developed a tabular void fraction prediction method based on X_{tt} and a property index related to viscosity and density. Tandon (1985), Premoli (1971), and Hughmark (1962) added additional factors to X_{tt} for void fraction modeling. Tandon’s model adds an additional single phase Reynolds number dependence. Premoli added a Weber number dependence as well as a Reynolds number dependence. Hughmark used a two-phase Reynolds number and a slight Froude number dependence in an implicit void fraction model.

A general observation relative to smooth tube, refrigerant void fraction data is that evaporator conditions can be reasonably modeled by a variety of standard void fraction correlations (e.g., Smith (1969), Wallis (1969) and Premoli (1971) were among the best). Condenser conditions, however, were poorly represented by all of these models. The primary feature distinguishing condensers is the relatively high vapor density, which is the result of the high pressure on the condenser side of refrigeration systems. At a given mass flux and quality, the vapor velocity in a condenser is slower than the velocity in an evaporator. Lower velocities drop the flow closer to the stratified flow region. In this region, void fraction predictions by any of the common void fraction models are inaccurate. A primary characteristic of flows near the stratified region is a strong void fraction dependence on refrigerant mass flux.

The border between the stratified and annular region is often pictured as a sharp line on flow maps (Taitel-Dukler 1976). The transition between the regions, however, is gradual. As vapor velocities increase, liquid moving along the bottom of a tube in “sewer pipe” flow gradually moves up the sidewall of a tube in a very non-uniform annular flow condition. This non-uniform film is very important in highly zeotropic refrigerant characteristics. Hurlburt and Newell (1997) developed a theoretical model for predicting the thickness profile of the liquid film as one moves from stratified to annular flow conditions.

In terms of void fraction prediction, refrigerant conditions spanning the stratified to annular regions must account for the amount of energy that is lost to gravitational effects that are “pumping” liquid refrigerant up the sidewalls of the tube. The models described by Rice (1987) rely primarily on inertial-inertial drag effects between the phases that are characteristic of the intermittent flow region (homogeneous models), or on inertial-viscous drag effects that are characteristic of the annular flow region (Lockhart-Martinelli models). Graham, et al. (1998b) introduced a new term for void fraction modeling, representing the ratio of the vapor kinetic energy relative to the energy required to pump liquid from the bottom of a tube to the top of a tube. The parameter was derived from the film thickness model of Hurlburt and Newell (1997) and is essentially a Froude number multiplied by a square root ratio of the vapor to liquid mass flow rates. The “Froude rate” parameter is:

$$F_t = \text{Froude Rate} = \left[\frac{G^2 x^3}{(1-x)\rho_g^2 g D} \right]^{0.5} \quad (4)$$

The stratified to annular flow region represents an area of operation that is spanned by most refrigerant systems as refrigerant is evaporated or condensed. As such, the common refrigerant flow conditions transit from gravitational drag dominated to viscous drag dominated effects. Recognizing that the Lockhart-Martinelli parameter is essentially a ratio of viscous drag effects to the vapor kinetic energy, and that the Froude rate parameter is a ratio of the vapor's kinetic energy to gravitational drag effects, a simple construction for modeling void fraction follows Wallis' (1969) viscous-only model.

$$\alpha = \text{function}(1/F_t + X_{tt}) = (1 + 1/F_t + X_{tt})^{-0.321} \quad (5)$$

Common evaporator conditions can be reasonably well represented by a correlation based on only the Lockhart-Martinelli parameter. Condenser conditions, however, are not represented well by the Lockhart-Martinelli parameter, but instead, are correlated well by the Froude rate parameter. The simple combined construction of the two effects unifies the drag terms and allows generalization of void fraction prediction over a broad range of refrigerant conditions. Graham, et al. (1998a) gives a detailed description of these effects for smooth tubes.

EXPERIMENT FACILITIES AND MEASUREMENT TECHNIQUES

Two different facilities were employed, one for evaporation tests and the other for condensation experiments. A more detailed explanation for the condenser appears in Graham, et al. (1998b) and Kopke, et al. (1998), and for the evaporator by Wilson, et al. (1998) and Yashar, et al. (1998). Though the systems used for evaporation and condensation experiments are different facilities, there are many similarities with the differences being related to the different test section inlet temperatures required.

Liquid refrigerant was moved by a pump through a mass flow meter and then to a "pre-heater". The pre-heater consisted of electric heater strips that were used to set the inlet quality. The refrigerant enters the test section after the pre-heater section. The refrigerant passes through a condensing section, and then back to the pump.

Cool water flowed in a counterflow direction on the outside of the test sections for condensation experiments. A refrigerant inlet temperature of 35°C was maintained for all condensation experiments. The evaporator test loop maintained a refrigerant inlet temperature of 5°C. Inlet quality was varied from almost pure liquid (5%) to nearly pure vapor (80%) in the tests. The lower bound of quality was chosen due because void fraction at 0% quality is known ($\alpha = 0.0$) thus 5% quality is assumed to be a reasonable level to begin testing. At the higher quality end the void fraction is also known at 100% quality ($\alpha = 1.0$) and void fractions for 80% quality were normally 0.9 and above and thus a reasonable level to stop determining void fraction. The mass flux was varied from 75 kg/m²·s to 700 kg/m²·s.

Type T thermocouples were used for temperature measurement are accurate within 0.2°C along the length of each test section. Instream thermocouples were placed ahead of the test section and after the test section outside of the shutoff valves. Thermocouples were soldered into grooves cut in copper sleeves at four circumferential locations (top, bottom, and sides) on the test section. The circumferential test section wall thermocouple measurements were made at four locations along the length of the test section. Wattelet (1994) and Dobson (1994) describe the thermocouple mounting procedure in more detail. Pressure transducers located in both loops

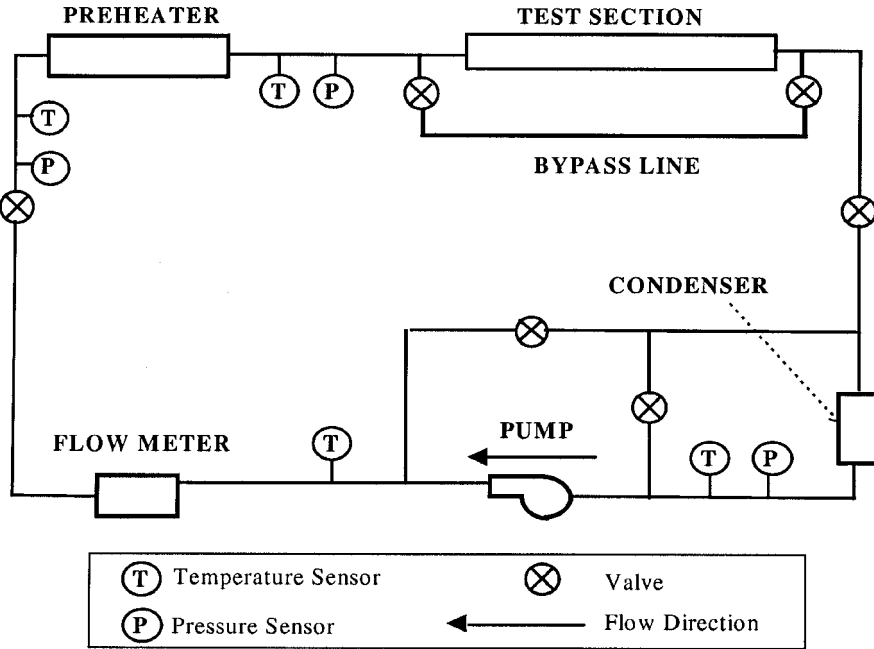


Figure 1. Schematic of condensation and evaporation flow loops

Table 1. Microfin Tube Specifications

Int. Base Diameter, mm	Helix, degrees	Number of Fins	Cross-Section, mm ²	Perimeter, mm
7.3	0	50	40.2	36.4
8.9	0	60	60.9	45.3
7.3	18	50	39.4	35.1
8.9	18	60	60.6	46.9

are accurate to 0.3% of the full scale reading. Electric power measurements use power transducers that are accurate to within 0.2% of their full scale reading. Mass flow measurements use either a Coriolis-type mass flow meter or a positive displacement volumetric flow rate meter.

The test sections are single pass cylindrical tubes with inside diameters of 7.3 mm and 8.9 mm approximately 1.2 m long. Specially made 0 degree tubes were obtained that closely matched the fin profile of commercially available 18 degree helix angle tubes at each diameter. Table 1 gives detailed information on the tube geometries. Figure 2 is a schematic of the larger 18 degree microfin tube. Evaporation tests were conducted on all four tubes. Condensation tests were made on the 8.9 mm diameter tubes with 0 degree and 18 degree helix angles. Fin height for all tubes is 0.2 mm.

A small diameter tap (approximately 1 mm inside diameter) machined from brass was soldered to the test section tube for refrigerant removal. Shutoff valves are located at opposite ends of the test section and a mechanical linkage connects the shutoff valve handles. The shutoff valves are ball valves with an internal port diameter similar to the test section tube diameter. The linkage allows simultaneous shutoff of the test section for trapping the fluid. A bypass line is opened when the test section is closed in order to keep the loop operating. Detailed descriptions of each test section and special fittings can be found in Graham, et al. (1998b); Kopke, et al. (1998); Wilson, et al. (1998); and Yashar, et al. (1998).

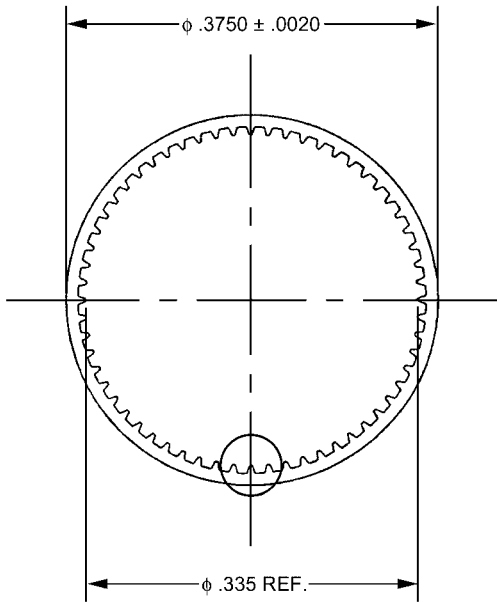


Figure 2. Schematic of the 8.9 mm diameter microfin tube geometry

Measurement Techniques and Procedures

Measurement of the void fraction required a known test section volume. While smooth tube volumes can be calculated from the tube geometry, microgrooved tube volume and the volume of special fittings for fluid removal and pressure measurement have volumes that are not easily calculated. A procedure for experimentally determining *in situ* test section volume was used to verify calculated volumes. First, the system was evacuated, and then the test section shutoff valves were closed. Next, a small receiver tank (approximately 1 litre in volume) was filled with either nitrogen, R134a, or R22 gas. The receiving tank was weighed to determine the amount of gas mass in the tank (with ± 0.01 gram resolution). The tank was then attached to the system via the void fraction tap, and the gas in the tank was then allowed to enter the test section. Temperature and pressure of the test section were recorded. The tank was

disconnected from the test section and weighed again to determine how much mass was released into the test section. Using the temperature and pressure of the gas in the test section allowed the gas specific volume to be determined. The volume of the test section was found by multiplying the mass injected into the test section by the specific volume. The three gases used over a range of receiver tank pressures gave good agreement in volume. Details and results of the procedure are described by Graham, et al. (1998b).

The void fraction measurement technique is one that has been commonly used by others (Hetsroni 1982). To make a void fraction measurement, the shutoff valves on either side of the test section were closed simultaneously, and the bypass line was opened. Pressure transducer lines were closed prior to closing the test section shutoff valves. A valve on the void fraction tap connecting the test section to an evacuated receiver tank was opened, allowing the refrigerant to flow out of the test section and into the tank. The tank was usually cooled and the test section was warmed (on the evaporator) to speed up the process. Once the refrigerant mass had migrated to the receiver tank, the temperature and pressure of the test section were recorded and the void fraction tap valve was closed.

The amount of mass that migrated into the receiving tank was weighed. The vapor mass left in the test section was determined from the temperature, pressure and volume. The mass in the test section was usually much less than five percent of the mass in the receiver tank. Once the total mass was known, the two-phase specific volume and void fraction of the test section was calculated.

Common sources of error in the experiments are leaks. Refrigerant can leak from loose fittings and improperly soldered joints, resulting in lower than actual amounts of mass in the receiving tank. Also, leaks across the shutoff valves can add refrigerant mass to the receiving tank. Performed properly, this method gave consistent mass readings to within 0.5 gram (usually less than 5% of test section mass) and void fractions to within 3% at a given condition.

Uncertainty Analysis

Following the uncertainty analysis presented by Tran (2000), the test section volume was determined to within 7%. With a mass reading uncertainty of 5%, the void fraction was calculated to within 9%. Experimentally the void fraction tests were repeated with an uncertainty of 3%, therefore the total uncertainty in the void fraction is approximately 10%.

R134a and R410A Refrigerant Properties

The two refrigerants used for the investigation give a range of properties that are representative of other refrigerants in the mid-pressure to high pressure refrigerant operation range. Table 2 lists properties of R134a and R410A over the range of conditions investigated. The properties were determined from REFPROP, computer software for refrigerant property determination (NIST 1993).

R410A is a "near" azeotropic 50/50 mass mixture of refrigerants R32 and R125. The saturation pressure given in the table is the liquid saturation pressure. The vapor saturation pressure is approximately 3 to 7 kPa higher than the liquid saturation pressure over the temperature range investigated.

Table 2. Refrigerant Properties at Test Conditions

Refrigerant	T , °C	P , kPa	Vapor Density, kg/m ³	Vapor Viscosity, μP	Liquid Density, kg/m ³	Liquid Viscosity, μP
R134a	5	349	16.9	112	1277	2688
R134a	35	888	42.6	128	1165	1884
R410A	5	931	34.4	122	1174	1621
R410A	35	2127	82.5	145	1031	1079

EXPERIMENT RESULTS AND DISCUSSION

Microfin void fraction characteristics generally follow trends observed in smooth tubes. In this section, the basic characteristics are discussed and the effects of mass flux, heat flux, heat flow direction, microfin geometry, and refrigerant are presented.

Figures 3 through 6 show the effect of mass flux on void fraction in microfin tubes. Figures 3 and 4 show void fraction variation under evaporation conditions. Figure 3 presents results from the 7.3 mm tube with 0 degree helix using R410A as the refrigerant. Figure 4 shows similar results for evaporation in the larger 8.9 mm tube with an 18 degree helix using R134a as the refrigerant. The common feature of these two plots is the relative insensitivity of void fraction to mass flux. Figures 5 and 6 show mass flux effects for condensation conditions. Both results are for the 8.9 mm tube with 18 degree microfin tube. Both figures show that condensation conditions display a void fraction dependency on mass flux. As discussed in the background section, high pressure in condensers results in vapor densities that reduce the vapor velocity for a given mass flux. The reduced vapor velocity of a condenser causes lower void fractions than found in evaporators at similar mass flux/quality conditions. Generally, condensers with mass fluxes above 200 kg/m²·s show less void fraction sensitivity to mass flux.

Figures 7 and 8 show the effect of heat flux level on evaporation void fraction. Similar to smooth tube results, no significant heat flux effect was found for either R134a or R410A over a 0 to 10 kW/m² heat flux range. The condenser experiment did not allow heat flux control due to water jacket cooling for heat removal. During smooth tube experiments, the condensation test loop was temporarily modified to allow heated water to evaporate refrigerant in the test section. The result of this experiment showed the condensing void fraction to be independent of heat flux and heat flow direction.

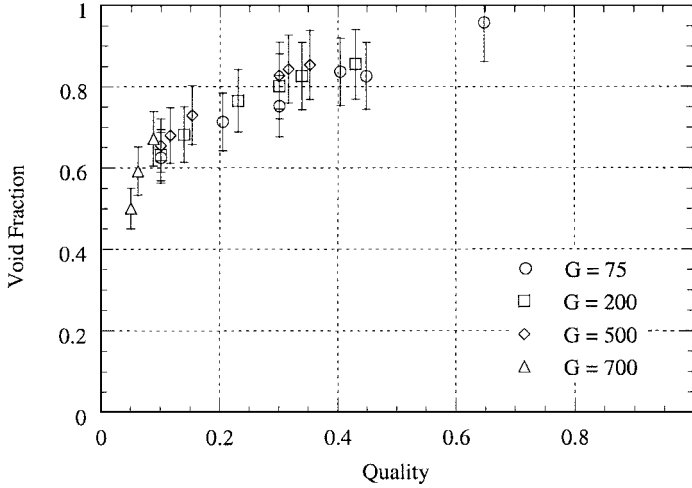


Figure 3. Void fraction variation of R410A in a 0 degree, 7.3 mm diameter microfin tube in evaporation. Mass fluxes ($\text{kg}/\text{m}^2\cdot\text{s}$) are given in the legend.

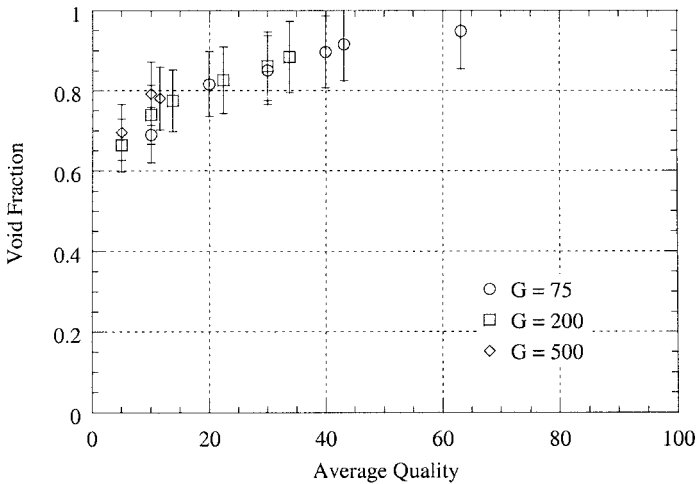


Figure 4. Void fraction variation of R134a in an 18 degree, 8.9 mm diameter microfin tube in evaporation. Mass fluxes ($\text{kg}/\text{m}^2\cdot\text{s}$) are given in the legend.

Figure 9 compares evaporation void fraction data collected from a 6.1 mm smooth tube and an 8.9 mm tube with an 18 degree helix angle. Data from refrigerants R134a and R410A are included on the plot. The primary observation from the figure is that tube diameter and microfin effects for evaporation tend to be less significant than refrigerant property variations. R410A with a relatively high vapor pressure, has lower vapor velocities than R134a at a given mass flux/quality condition, thus leading to lower void fractions. During smooth tube (4.3 mm to 8.9 mm in diameter) testing, void fraction was found to be insensitive to tube diameter variation. Tubes with diameters less than 4.3 mm may have different void fraction trends as microchannel flow behavior (possibly an intermittent-type flow) becomes significant.

Figure 10 compares results for the 8.9 mm diameter, 0 degree and 18 degree helix angle tubes in evaporation for refrigerants R134a and R410A. No significant differences due to helix angle

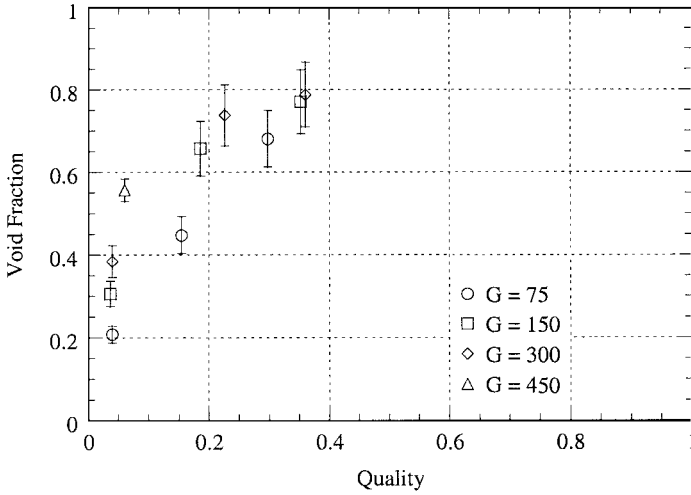


Figure 5. Void fraction variation of R134a in an 18 degree, 8.9 mm diameter microfin tube in condensation. Mass fluxes ($\text{kg/m}^2\cdot\text{s}$) are given in the legend.

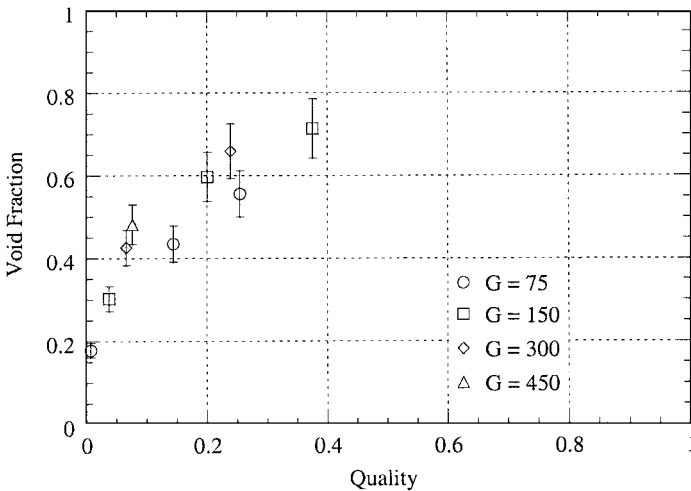


Figure 6. Void fraction variation of R410A in an 18 degree, 8.9 mm diameter microfin tube in condensation. Mass fluxes ($\text{kg/m}^2\cdot\text{s}$) are given in the legend.

were observed in the results, although, the two tubes are known to have significant differences in heat transfer characteristics [Chiang (1993), Graham, et al. (1999)]. However, as shown by Graham, et al. (1999), axial and helically grooved tubes have similar pressure drop characteristics. Pressure drop characteristics are important indicators of void fraction characteristics because both factors are related to the flow energy dissipation rate. Similar to the comparison in Figure 9 between smooth and microfin tubes, the primary void fraction dependency observed in Figure 10 is related to refrigerant properties.

Figures 11 and 12 characterize the trends in void fraction relative to the dimensionless Lockhart-Martinelli and Froude rate parameters. As previously discussed, lower vapor velocity conditions tend to be in the stratified-wavy flow region while higher vapor velocity conditions are

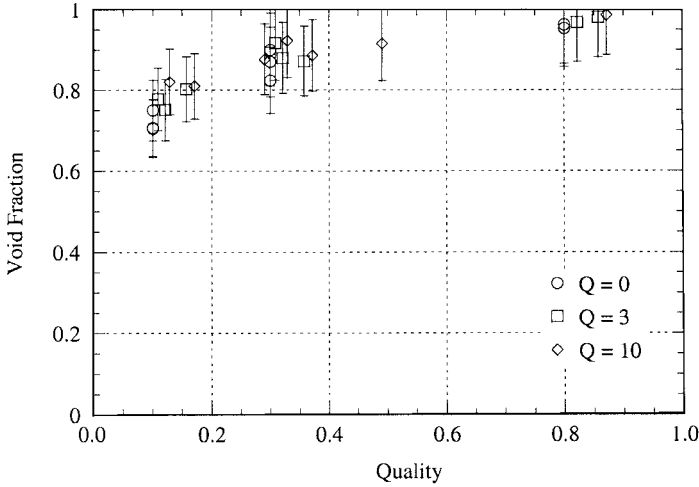


Figure 7. R134a void fraction over a range of evaporation heat fluxes (0 to 10 kW/m²) in a 0 degree, 8.9 mm diameter microfin tube. Heat fluxes (kW/m²) are given in the legend.

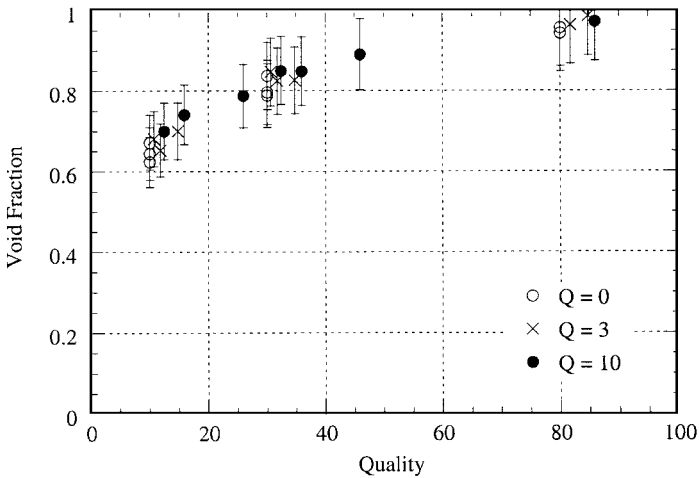


Figure 8. R410A void fraction over a range of evaporation heat fluxes (0 to 10 kW/m²) in a 0 degree, 8.9 mm diameter microfin tube. Heat fluxes (kW/m²) are given in the legend.

in the annular flow region. The Froude rate parameter becomes a significant factor describing the flow field energy dissipation by the gravitational lifting and falling of waves in the liquid. The Lockhart-Martinelli parameter describes the flow energy dissipation processes in the annular flow region due to interaction between the vapor and liquid. Figure 11 shows the condensation data while Figure 12 shows the evaporation data. In Figure 11, the Froude rate shows somewhat better correlation of data than the Lockhart-Martinelli parameter. Figure 12, on the other hand, shows the evaporator data to be correlated better by the Lockhart-Martinelli parameter, indicating the relative independence of annular flow from gravitational effects.

Overall, both gravitational and liquid-vapor viscous interaction effects are important, requiring some combination of these effects for overall modeling of the annular to stratified flow

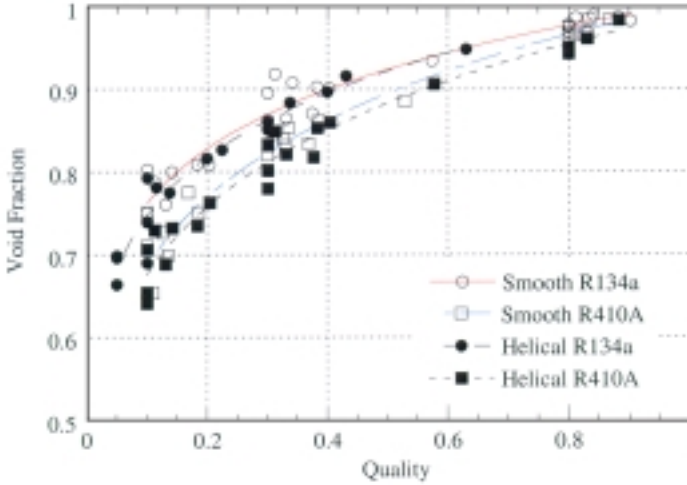


Figure 9. Comparison of void fraction effects in a 6.9 mm smooth and 8.9 mm 18 degree microfin tube for refrigerants R134a and R410A in evaporation. Void fraction error bars are at 10% of void fraction value

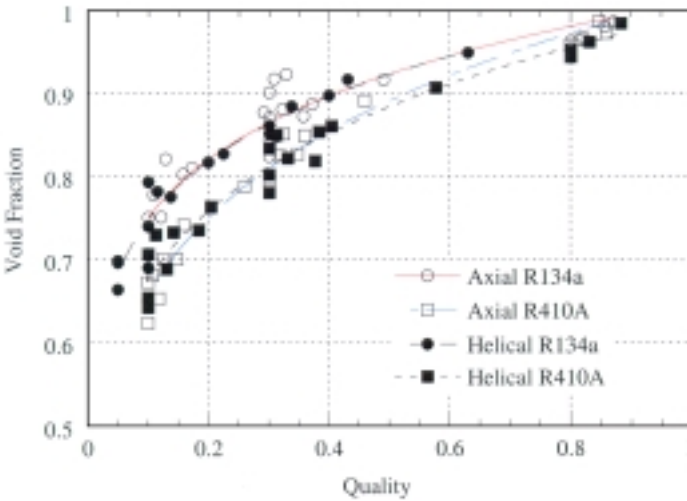


Figure 10. Comparison of void fraction effects for 0 degree and 18 degree, 8.9 mm diameter microfin tubes with refrigerants R134a and R410A in evaporation. Void fraction error bars are at 10% of void fraction value.

regions. A simple construction used for correlating smooth tube void fraction results is the summation of the Lockhart-Martinelli parameter and the reciprocal Froude rate parameter (Graham, et al. 1998a). This combination, as previously discussed, is the ratio of the dissipative effects to the flow kinetic energy. No scaling has been assumed in the simple construction represented by equation (5), and the two dissipative effects are assumed to act in an independent manner. Figure 13 shows a plot of all of the microfin tube void fraction data (condensation and evaporation, axial and 18 degree helix angles) as a function of the combined flow field dissipation parameter.

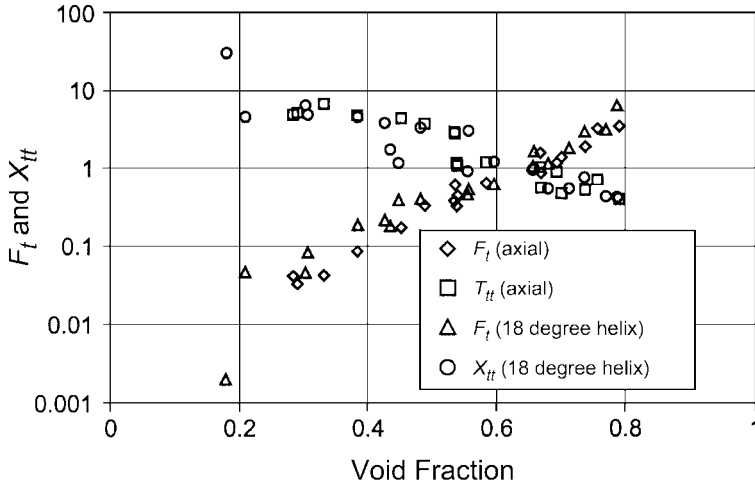


Figure 11. Axial and 18 degree helical microfin condenser void fraction data plotted vs. the Lockhart-Martinelli parameter and the Froude rate parameter.

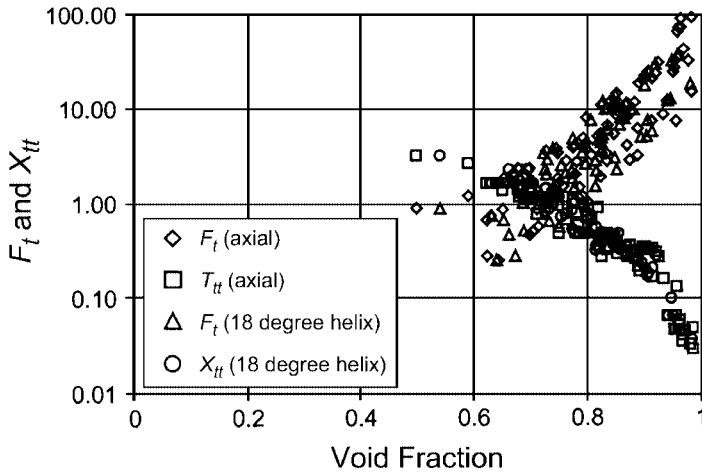


Figure 12. Axial and 18 degree helical microfin evaporator void fraction data plotted vs. the Lockhart-Martinelli parameter and the Froude rate parameter.

As shown in Figure 13, the microfin condensation data is displaced relative to the predictions. The line labeled “Smooth Tube” in Figure 13 represents the void fraction prediction of equation (5) for smooth tube results. No differences in smooth tube void fraction trends were observed between evaporation and condensation data. In microfin tubes, however, condensation results for both axial and 18 degree helical microfins show a decrease in void fraction from the smooth tube results and from the evaporation microfin void fraction results. A dashed curve has been plotted on Figure 13 using equation (5) with an exponent value of -0.375 . The evaporation microfin results tend to show good agreement with the smooth tube void fraction prediction of equation (5). The microfin condensation void fraction data is approximately 0.05 less than the smooth tube void fraction, which is approximately the fraction of cross-section area contained in

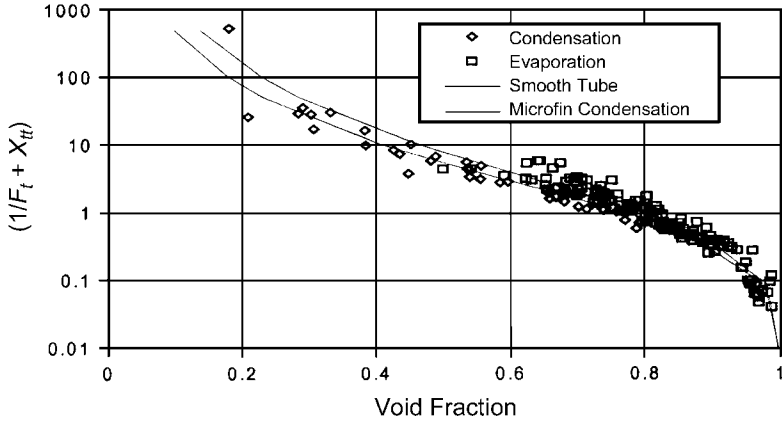


Figure 13. Axial and 18 degree helical microfin void fraction (evaporation and condensation) data plotted versus the sum of the Lockhart-Martinelli and reciprocal Froude rate parameters.

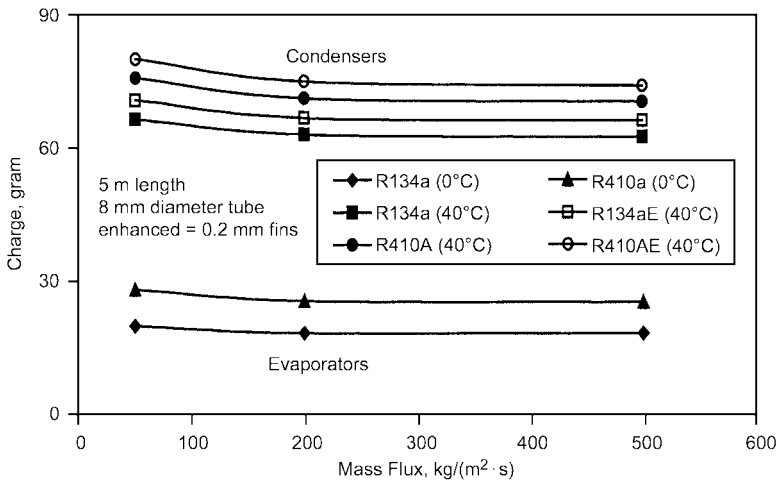


Figure 14. Refrigerant charge prediction for smooth and microfin tubes in evaporation and condensation.

the groove regions. Possibly, the void fraction decrease in condensation is due to fluid collecting in the groove regions around the tube periphery while microfin tubes in evaporation tend to form a liquid film profile around the tube in a manner similar to smooth tubes.

One of the most useful features of the void fraction parameter is the prediction of refrigerant charge. Locally, the refrigerant charge per tube length is:

$$= A \{ \alpha \rho_g + (1 + \alpha) \rho_l \} \tag{6}$$

Figure 14 shows the estimated charge for a 5 meter long, 8 mm diameter tube with refrigerants R134a and R410A in evaporation and condensation. Refrigerant condenser conditions with the “E” designation in Figure 14 represent enhanced tubes. The evaporation process is assumed

to change linearly from a quality of 0.2 to 1.0 over the tube length at a saturation temperature of 0°C. The condenser process is assumed to change linearly from a quality of 1.0 to 0.0 at a saturation temperature of 40°C. At low mass fluxes, where vapor velocities are reduced causing the flow to transition into a stratified flow, an increase in refrigerant charge is observed. For condensers with microfin tubes, the effect of the decreased void fraction is observed. Overall, the condenser tubes tend to have a higher charge requirement than evaporator tubes at similar mass fluxes. Also, higher pressure refrigerants require higher refrigerant charges than lower pressure refrigerants at similar mass flux conditions.

CONCLUSIONS

Void fraction results for microfin tubes generally show trends that are similar to smooth tubes. Microfin tube evaporation results have shown relative insensitivity to mass flux and heat flux levels. Microfin tube condensation results have shown a reduced void fraction at conditions similar to smooth tubes at the same mass flux and quality conditions. The reason for the void fraction reduction is unknown. No significant differences in void fraction due to helix angle for the 0 degree and 18 degree helix angle tubes were observed. Simple expressions for determining void fraction and refrigerant charge per length in smooth and microfin tubes have been presented.

ACKNOWLEDGEMENTS

The authors express their gratitude to the University of Illinois Air Conditioning and Refrigeration Center, an NSF sponsored/industry supported research center, for financial support of this project.

NOMENCLATURE

A = tube cross-section area (m^2)

C = charge per tube length (kg/m)

D = tube diameter (mm)

F_f = Froude rate parameter = $\left[\frac{G^2 x^3}{(1-x)\rho_g^2 g D} \right]^{0.5}$

g = gravitational acceleration (m/s^2)

G = mass flux (kg/m^2s)

S = slip velocity ratio = vapor velocity/liquid velocity

x = quality = vapor mass flow rate/total mass flow rate

X_{tt} = Lockhart-Martinelli parameter

$\left(\frac{1-x}{x} \right)^{0.9} \left(\frac{\rho_g}{\rho_l} \right)^{0.5} \left(\frac{\mu_l}{\mu_g} \right)^{0.1}$

α = void fraction = vapor volume/total volume

ρ_g = vapor density (kg/m^3)

ρ_l = liquid density (kg/m^3)

μ_g = vapor dynamic viscosity ($kg/m \cdot s$)

μ_l = liquid dynamic viscosity ($kg/m \cdot s$)

REFERENCES

- Ahrens, F.W. 1983. Heat Pump Modeling, Simulation and Design. Proc. of the NATO Advanced Study Inst. on Heat Pump Fundamentals, Espinho, Spain 1980: J. Berghmans, Ed. Martinus Nijhoff Publishers.
- Bankoff, S.G. 1960. A Variable Density Single-fluid Model for Two-Phase Flow with Particular Reference to Steam-Water Flow. Transactions ASME, *J. of Heat Transfer* 82: 265-72.
- Baroczy, C.J. 1965. Correlation of Liquid Fraction in Two-Phase Flow with Application to Liquid Metals. Chemical Engineering Progress Symposium Series 61(57): 179-91.
- Chiang, R. 1993. Heat Transfer and Pressure Drop during Evaporation and Condensation of Refrigerant 22 in 7.5 mm and 10 mm Diameter Axial and Helical Grooved Tubes. Proc. *AIChE Heat Transfer Symposium* 89(295): 205-10.
- Collier, J.G. 1980. *Convective Boiling and Condensation*. 2nd Ed., McGraw-Hill: 37-54.
- Dobson, M.K. 1994. Heat Transfer and Flow Regimes during Condensation in Horizontal Tubes. *Ph.D. Thesis*, University of Illinois, Urbana-Champaign, IL.
- Domanski, P., and Didion, D. 1983. Computer Modeling of the Vapor Compression Cycle with Constant Flow Area Expansion Device. NBS Building Science Series 155.

- Graham, D.M., H.R. Kopke, M.J. Wilson, D.A. Yashar, J.C. Chato, and T.A. Newell. 1998a. An Investigation of Void Fraction in the Stratified/Annular/Intermittent Flow Regions in Smooth, Horizontal Tubes. ACRC TR-144, Air Conditioning and Refrigeration Center, University of Illinois, Urbana-Champaign, IL.
- Graham, D.M., T.A. Newell, and J.C. Chato. 1998b. Experimental Investigation of Void Fraction during Refrigerant Condensation. ACRC TR-135, Air Conditioning and Refrigeration Center, University of Illinois, Urbana-Champaign, IL.
- Graham, D.M., J.C. Chato, and T.A. Newell. 1999. Heat Transfer and Pressure Drop during Condensation of Refrigerant 134a in an Axially Grooved Tube, *Intl J. of Heat and Mass Transfer* 42: 1935-1944.
- Hetsroni, G. 1982. *Handbook of Multiphase Systems*: Hemisphere Publishing Corp., 10.24-10.26.
- Hughmark, G.A. 1962. Holdup in Gas-Liquid Flow. *Chemical Engineering Progress* 58(4): 62-65.
- Hurlburt, E.T. and T.A. Newell. 1997. Modeling of the Evaporation and Condensation of Zeotropic Refrigerant Mixtures in Horizontal, Annular Flow. ACRC TR-129, Air Conditioning and Refrigeration Center, University of Illinois, Urbana-Champaign, IL.
- Hurlburt, E.T. and T.A. Newell. 1999. Characteristics of Refrigerant Film Thickness, Pressure Drop, and Condensation Heat Transfer in Annular Flow. *HVAC&R Research*, 5(3): 229-248.
- Kopke, R.K., T.A. Newell, and J.C. Chato. 1998. Experimental Investigation of Void Fraction during Refrigerant Condensation in Horizontal Tubes. ACRC TR-142, Air Conditioning and Refrigeration Center, University of Illinois, Urbana-Champaign, IL.
- Levy, S. 1960. Steam Slip Theoretical Prediction from Momentum Model. *Transactions ASME, J. of Heat Transfer*, Series C 82: 113-124.
- Lockhart, R.W. and R.C. Martinelli. 1949. Proposed Correlation of Data for Isothermal Two-Phase, Two-Component Flow in Pipes. *Chemical Engineering Progress* 445(1): 39-48.
- Newell, T.A. and ?? Shah, 1999. Refrigerant Heat Transfer, Pressure Drop, and Void Fraction Effects in Microfin Tubes, 2nd International Symposium on Two-Phase Flow 1 Modelling and Experimentation, Pisa, Italy, also to appear in April 2001 *HVAC&R Research* .
- NIST 1993. NIST Thermodynamic Properties of Refrigerants and Refrigerant Mixtures. Version 4.01: Computer software, National Institute of Science and Technology, Gaithersburg, MD.
- Premoli, A., Francesco, D., and Prina, A. 1971. A Dimensional Correlation for Evaluating Two-Phase Mixture Density. *La Termotecnica* 25(1): 17-26.
- Rice, C.K. 1987. The Effect of Void Fraction Correlation and Heat Flux Assumption on Refrigerant Charge Inventory Predictions. *ASHRAE Transactions* 93, Part 1: 341-67.
- Sacks, P.S. 1975. Measured Characteristics of Adiabatic and Condensing Single Component Two-Phase Flow of Refrigerant in a 0.377 in. Diameter Horizontal Tube. ASME Winter Annual Meeting, 75-WA/HT-24, Houston, Texas.
- Smith, S.L. 1969. Void Fractions in Two-Phase Flow: A Correlation Based Upon an Equal Velocity Head Model. *Proc. Instn. Mech. Engrs.*, 184, Part 1(36): 647-64.
- Taitel, Y. and A.E. Dukler. 1976. A Model for Predicting Flow Regime Transitions in Horizontal and Near Horizontal Gas-Liquid Flow. *AIChE Journal* 22: 45-55.
- Tandon, T.N., H.K. Varma, and C.P. Gupta. 1985. A Void Fraction Model for Annular Two-Phase Flow. *Int. J. Heat and Mass Transfer* 28(1): 191-98.
- Thom, J.R.S. 1964. Prediction of Pressure Drop during Forced Circulation Boiling of Water. *Int. J. Heat and Mass Transfer* 7: 709-24.
- Tran C.C. 2000. A Study of Refrigerant Void Fraction and Pressure Drop in Return Bends and Development of a New Two-Phase Experimental Apparatus, *M.S. thesis*, University of Illinois, Urbana, IL.
- Traviss, D.P., W.M. Rohsenow, and A.B. Baron. 1973. Forced Convection Condensation Inside Tubes: A Heat Transfer Equation for Condenser Design. *ASHRAE Transactions* 79, Part 1: 157-65.
- Wallis, G.B. 1969. *One-Dimensional Two-Phase Flow*: McGraw-Hill, 51-54.
- Wilson, M.J., T.A. Newell, and J.C. Chato. 1998. Experimental Investigation of Void Fraction during Horizontal Flow in Larger Diameter Refrigeration Applications. ACRC TR-140, Air Conditioning and Refrigeration Center, University of Illinois, Urbana-Champaign, IL.
- Wattelet, J.P. 1994. Heat Transfer Flow Regimes of Refrigerants in a Horizontal-Tube Evaporator. *Ph.D. Thesis*, University of Illinois, Urbana-Champaign, IL.

- Yashar, D.A., T.A. Newell, and J.C. Chato. 1998. Experimental Investigation of Void Fraction during Horizontal Flow in Smaller Diameter Refrigeration Applications. ACRC TR-141, Air Conditioning and Refrigeration Center, University of Illinois, Urbana-Champaign, IL.
- Zivi, S.M. 1964. Estimation of Steady-State Steam Void-Fraction by Means of the Principle of Minimum Entropy Production. Transactions ASME, *J. of Heat Transfer Series C*, 86: 247-52.